

## Crystallization Kinetics and Morphology of Poly(3-hydroxybutyrate)/Cellulose Ester Blends

Maria Pizzoli, Mariastella Scandola,\* and Giuseppina Ceccorulli

Dipartimento di Chimica "G. Ciamician" della Università di Bologna and Centro di Studio per la Fisica delle Macromolecole del CNR, Via Selmi 2, 40126 Bologna, Italy

Received February 25, 1994; Revised Manuscript Received May 12, 1994\*

**ABSTRACT:** Isothermal crystallization from the melt of blends of bacterial poly(3-hydroxybutyrate) (PHB) with two cellulose acetobutyrate (CE1 and CE2) has been investigated by hot-stage optical microscopy. Space-filling spherulites are observed at all compositions (50–100% PHB) and crystallization temperatures (50–130 °C) explored. The spherulite radius increases linearly with time, and the radial growth rate ( $G$ ) strongly depends on the cellulose ester content of the blend.  $G$  decreases with increasing CE content: the crystallization rate of the blend containing 50% CE2 is 2.5 orders of magnitude lower than that of pure PHB. The spherulites show banding whose spacing increases with increasing  $T_c$  for a given blend, while at constant  $T_c$  banding decreases with increasing cellulose ester concentration. In PHB/CE1 blends, owing to the ability of CE1 to crystallize from the melt concomitantly to PHB at certain compositions and crystallization temperatures, a very unusual deviation from linearity of the radial growth of PHB spherulites is observed. The rate is seen to increase with time, reflecting the compositional changes which occur in the melt as a consequence of CE1 crystallization. Apart from the cases where crystallization of CE1 occurs, the morphology of melt-crystallized PHB/CE1 and PHB/CE2 blends is rather independent of the cellulose ester identity.

### Introduction

Recently, intensive fundamental and applied research<sup>1–4</sup> has been devoted to the study of bacterial poly(3-hydroxybutyrate) (PHB) and related poly(hydroxyalcanoates) (PHA). The homopolymer PHB as well as some copolymers is commercially available, and a number of applications in the marine, medical, and agricultural fields have been proposed on the basis of properties such as biocompatibility and environmental biodegradability. However, some physical properties of PHB—exceeding brittleness of the highly crystalline polymer, for example—are not satisfactory. In order to decrease brittleness and generally to improve properties, blending with a second polymeric component has been attempted by a number of investigators. A wide variety of polymers have been considered as components of binary blends with PHAs: hydrocarbons polymers,<sup>5</sup> polysaccharides,<sup>6</sup> aliphatic synthetic polyesters,<sup>7,8</sup> poly(ethylene oxide)<sup>9</sup> (PEO), poly(vinyl acetate)<sup>7,10</sup> (PVA), chlorinated polymers,<sup>11</sup> cellulose derivatives,<sup>12–15</sup> and poly(methacrylates).<sup>16</sup> Only a few of the blends investigated have been reported to be truly miscible, namely, those with PEO,<sup>9</sup> PVA,<sup>7,10</sup> and some cellulose esters<sup>12–15</sup> (CE). Miscibility in the melt over the whole composition range has been recently found<sup>12–15</sup> for both PHB and a bacterial 3-hydroxybutyrate/3-hydroxyvalerate copolymer containing 20 mol % of 3 HV units, with CEs having degrees of substitution (DS) in the range 2.7–3. In these blends the PHA, whose glass transition temperature ( $T_g$ ) is about 0 °C, acts as a high molecular weight plasticizer toward the high- $T_g$  cellulose derivative. As a consequence, the melt-quenched blends show a  $T_g$  which decreases with increasing PHA content from 0 to 50% in excellent agreement with the behavior predicted for totally miscible binary systems.<sup>17,18</sup> Conversely, at higher PHA contents, the blend  $T_g$  only slightly depends on composition, according to a well-documented behavior widely discussed in previous papers.<sup>12,14</sup> As expected for miscible blends containing crystallizable components, also the melting temperature ( $T_m$ ) changes with composition in PHA/CE blends. Hence, the width of the  $T_g$ – $T_m$  window varies, together with the capability of the component

polymers to crystallize out of the homogeneously mixed blend at  $T > T_g$ .

The polymers which constitute the blends investigated in the present paper show quite different crystallization behavior. Because of its biological origin, PHB is a 100% stereoregular polyester which develops a remarkably high crystalline fraction (typically about 60%). When isothermally crystallized from the melt, PHB forms regularly banded spherulites which can reach very large dimensions<sup>19</sup> (in appropriate conditions up to several centimeters) due to extremely low nucleation density. Optical microscopy has been successfully used to monitor PHB spherulite growth<sup>19,20</sup> over a wide range of temperatures. The cellulose esters, conversely, develop a nonspherulitic crystalline phase, whose randomly oriented microcrystals only contribute weak diffuse birefringence when observed through the crossed polars of an optical microscope. For this reason the kinetics of CE crystallization cannot be studied by optical microscopy.

When PHB/CE blends are allowed to crystallize isothermally from the melt, crystallization of the bacterial component can be easily followed by measuring the radial growth rate ( $G$ ) of PHB spherulites. It is known that spherulites grown at a constant temperature ( $T_c$ ) from a given miscible molten blend will show either a radius which increases linearly with time—indicating constancy of composition of the melt from which the polymer crystallizes—or, conversely,  $G$  will change with time calling for changes of melt composition. Substantially different morphologies are expected to develop in the blends as a consequence of different crystallization conditions.

The aim of the present work is to investigate the isothermal crystallization behavior of PHB/CE blends with varying composition, in order not only to quantify the retardation effect displayed by the high- $T_g$  cellulose component on the crystallization rate of the bacterial polyester but also to reveal the different morphologies which develop at each specific composition and crystallization temperature. Two blend systems, differing in the type of cellulose ester, have been taken into account. In both cases the CE content (in wt %) varied from 0 to 50. Optical microscopy was used to monitor crystallization over a broad range of temperatures (50–130 °C).

\* Abstract published in *Advance ACS Abstracts*, July 1, 1994.

**Table 1. Molecular Parameters of PHB and Cellulose Esters**

polymer	DS <sub>Bu</sub>	DS <sub>Ac</sub>	$M_n \times 10^{-3}$	$M_w \times 10^{-3}$	$T_g^a$ (°C)	$T_m^b$ (°C)
PHB			350	1140	4	175
CE1	2.58	0.36	61	130	103	188
CE2	2.50	0.18	71.6	161	119	

<sup>a</sup> By DSC after melt quenching; heating rate 20 °C/min. <sup>b</sup> By DSC, first scan at 20 °C/min.

## Experimental Section

**Materials.** Poly(3-hydroxybutyrate) (PHB; BXGV9) was kindly supplied by ICI Biological Products (U.K.). The cellulose esters (cellulose acetate butyrate) were commercial Eastman Kodak products: EAB 500-1 and CAB 531-1 (indicated throughout the paper as CE1 and CE2, respectively), whose degrees of substitution (DS) and molecular weights were kindly determined by Dr. C. Buchanan (Eastman Chemical Co., Kingsport, TN) by <sup>1</sup>H NMR and GPC in chloroform, respectively. Molecular weight, DS, and thermal properties are collected in Table 1.

Blends of PHB with the cellulose ester were prepared, as previously described,<sup>12</sup> by melt mixing at 195 °C in a miniature mixing/injection-molding machine followed by quenching in an ice-water mixture.

**Crystallization Measurements.** Measurements of the radial growth rate of spherulites were carried out with a Zeiss Axioscop polarizing optical microscope, equipped with a Linkham TH 600 hot stage. Isothermal crystallization measurements were performed on a thin slice of the injection-molded sample, inserted between two microscope cover glasses, and subjected to the following thermal program. The sample was heated at 20 °C/min up to 180 °C (where the melt was squeezed into a film through a small pressure applied to the upper glass) and then at 10 °C/min up to 200 °C. The heating step was followed by rapid quenching by means of N<sub>2</sub> gas flow (cooling rate > 250 °C/min) to the selected crystallization temperature, where isothermal crystallization was carried out. The whole procedure was performed without removing the sample from the hot stage. A videocamera, attached to the microscope through the Linkham VTO232 interface, allowed real time measurement of the spherulite dimensions, after calibration with a micrometric reticule. A video recording facility was used whenever crystallization was either too fast or too slow to be directly observed. A new sample was used for each crystallization measurement. Growth of four different spherulites (20–25 radius measurements each) was typically monitored at each  $T_c$ . When linear radius vs time behavior was obtained the correlation coefficient was always better than 0.999.

**X-ray Diffraction.** X-ray diffraction measurements were made with a Philips PW1050/81 powder diffractometer controlled by a PW1710 unit, using nickel-filtered Cu K $\alpha$  radiation ( $\lambda$  = 0.1542 nm; 40 kV; 30 mA).

## Results and Discussion

In order to facilitate the understanding of the crystallization kinetics of PHB/CE blends investigated in this work, Figure 1 summarizes previous results on the thermal behavior of blends of PHB with CE1<sup>12</sup> and CE2<sup>14</sup> over the whole range of compositions. The data reported were obtained by differential scanning calorimetry (DSC) measurements at 20 °C/min, on melt-quenched samples. As widely discussed in previous papers<sup>12,14</sup> the dependence on composition of the glass transition temperature ( $T_g$ ) of the blends is different according to the composition range considered: while at low PHB contents a strong dependence is observed,  $T_g$  is seen to change only slightly with composition when PHB becomes the major blend component. In these PHB-rich blends, the bacterial polymer is found to crystallize above  $T_g$  during the thermal scan in both PHB/CE systems considered. The crystallization process in the blends is somewhat retarded with respect to pure PHB (compare the crystallization temperatures,  $T_c$ , in Figure 1) and the crystalline phase so obtained melts

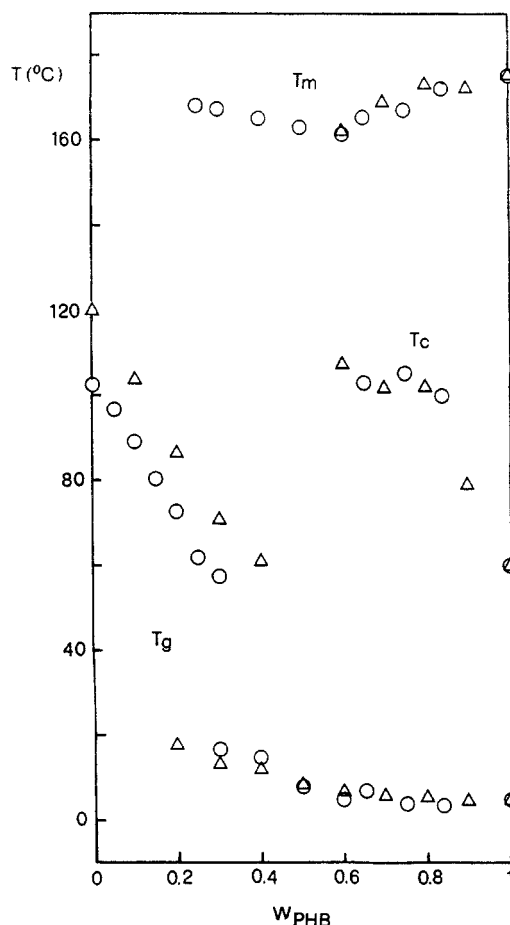


**Figure 1.** DSC results (melting temperature,  $T_m$ ; crystallization temperature,  $T_c$ ; glass transition temperature,  $T_g$ ) of melt-quenched PHB/CE1 (O) and PHB/CE2 ( $\Delta$ ) blends as a function of PHB weight fraction.

at a temperature which varies with blend composition as expected for binary miscible systems (compare the melting temperatures,  $T_m$ , in Figure 1). When PHB amounts to less than 60%, in the experimental conditions employed (heating rate 20 °C/min) no crystalline phase develops upon heating above  $T_g$  in PHB/CE2 blends, while in PHB/CE1 blends it is the cellulosic component which undergoes crystallization, as clearly indicated by the abrupt inversion of the  $T_m$ /composition dependence in Figure 1. The capability of CE1 to crystallize from PHB/CE1 blends—as opposed to the inability to do so in the same experimental conditions when in the pure state—was previously attributed<sup>12,13</sup> to widening of the  $T_g$ – $T_m$  window (i.e., the temperature interval available for crystallization) due to the “plasticizing effect” of PHB on the glass transition of the cellulose ester. Despite an analogous  $T_g$  decrease in PHB/CE2 blends (see Figure 1), no CE2 crystalline phase develops in such blends due to the inherent inability to crystallize of this lower DS cellulose ester.

Blends of PHB with CE1 and CE2 (CE content 0–50%) have been subjected to isothermal crystallization measurements in the hot stage of a polarizing optical microscope. Growth of PHB spherulites is observed at all temperatures and blend compositions investigated. Measurements of the spherulite radius ( $R$ ) as a function of time yield linear plots such as the ones reported in Figure 2 for a PHB/CE2 blend containing 80% PHB. It is seen that the slope of the straight lines, which represents the radial growth rate  $G$ , changes with  $T_c$ :  $G$  increases with  $T_c$  up to a maximum and then decreases, following a trend which is well-known in pure polymers. Only one of the blends, under certain circumstances, produced nonlinear

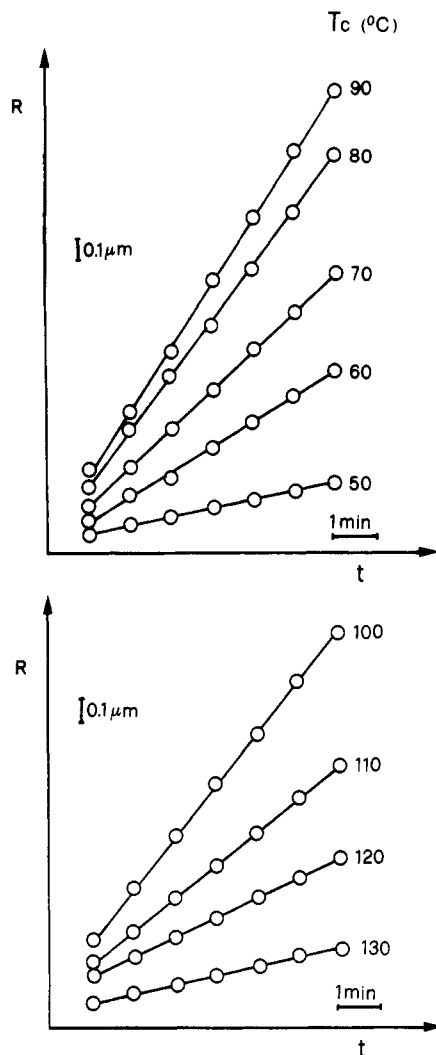


**Figure 2.** Spherulite radius  $R$  as a function of time for an 80/20 PHB/CE2 blend isothermally crystallized at different temperatures ( $T_c$ ).

$R$  vs  $T$  plots. This specific blend (PHB/CE1, 50/50) will be separately discussed in the following.

In blends, the rate of spherulite growth at a given temperature is primarily governed by the composition of the melt at the growing lamellar front and a steady-state growth indicates constancy of melt composition.<sup>21</sup> The linear dependences reported in Figure 2, which are representative of all but one of the PHB/CE blends investigated, imply that in the range of  $T_c$ s explored, while the growing PHB lamellae extract pure PHB from the mixed melt, the rejected high molecular weight cellulose ester does not migrate toward the molten mixed phase. The CE remains trapped in the immediate vicinity of the growing PHB crystals, into the space either between the lamellae (interlamellarly) or between bundles of lamellae (interfibrillarly), leaving the melt composition unchanged.

The presence of the second, high- $T_g$  component in the blends remarkably decreases the rate of PHB crystallization. Figure 3 shows the spherulite radial growth rate  $G$  as a function of  $T_c$  for PHB/CE1 and PHB/CE2 blends with different composition, together with the  $G$  vs  $T_c$  curve for pure PHB, for the sake of comparison. The rate is seen to decrease progressively with increasing CE content in both systems: by about 1 order of magnitude as the CE content reaches 20% by weight and as much as 2.5 orders of magnitude when CE2 concentration amounts to 50%.

To a first approximation, in miscible polymer blends where the crystallizable component is the low- $T_g$  polymer

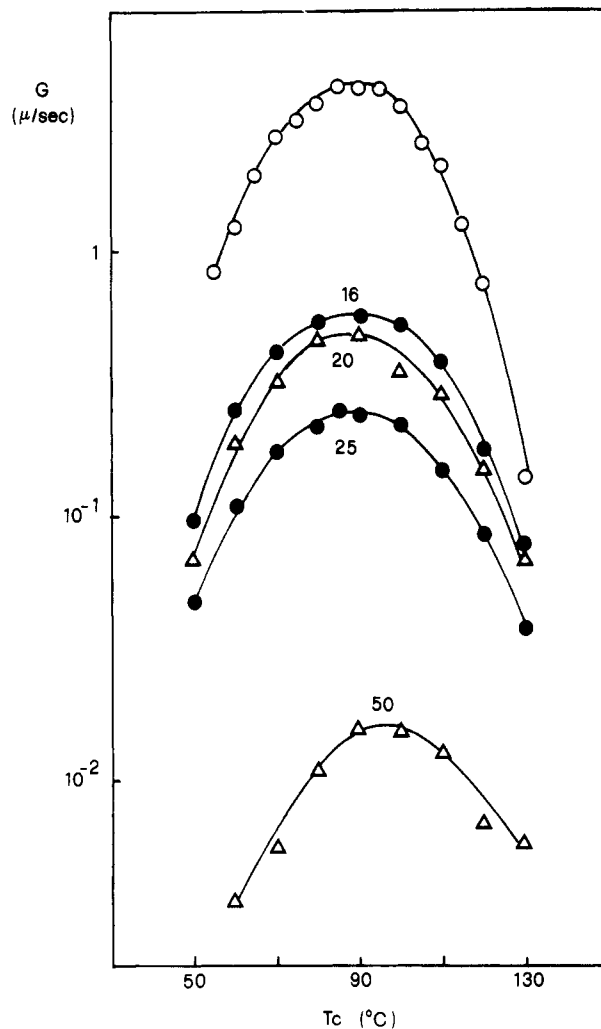


**Figure 3.** Radial growth rate ( $G$ ) as a function of  $T_c$  for PHB (○), PHB/CE1 blends (●) and PHB/CE2 blends (△). Number on curves: cellulose ester weight %.

three main factors can be taken into account to explain the crystallization rate depression observed: (a) a dilution effect which diminishes the number of crystallizable elements at the growing lamellar front; (b) a decrease of segmental mobility due to changes in  $T_g$  associated with the presence of the intimately mixed high- $T_g$  component; (c) a reduction of the driving force for crystallization due to melting point depression (decrease of undercooling).

Crystallization rate depressions of magnitude similar to the ones observed in Figure 3 have been reported<sup>22</sup> for miscible blends of poly(methyl methacrylate) (PMMA) with poly(vinylidene fluoride) (PVDF). In the PMMA/PVDF system the rate decrease was mainly attributed to changes in fluidity of the melt caused by large  $T_g$  changes with composition.<sup>22</sup> In regard to the PHB/CE systems under investigation, from the  $T_g$ /composition dependence of Figure 1 it is evident that  $T_g$  only slightly changes in the range of CE contents 0–25%; concomitantly, the melting temperature shows a decrease of less than 10 °C. Though the  $T_m$  reduction may play a role in determining the decrease of the crystallization rate of PHB in the blends, it is suggested that the remarkable rate depression observed is mainly associated with the dilution effect produced by the presence of the cellulosic component.

Since  $T_g$  and  $T_m$  represent respectively the lower and upper temperature limit to crystallization, the  $G$  vs  $T_c$  curves are expected to show little if any shift on the temperature scale, in the composition range 0–25% CE. As a matter of fact, the crystallization curves of such blends

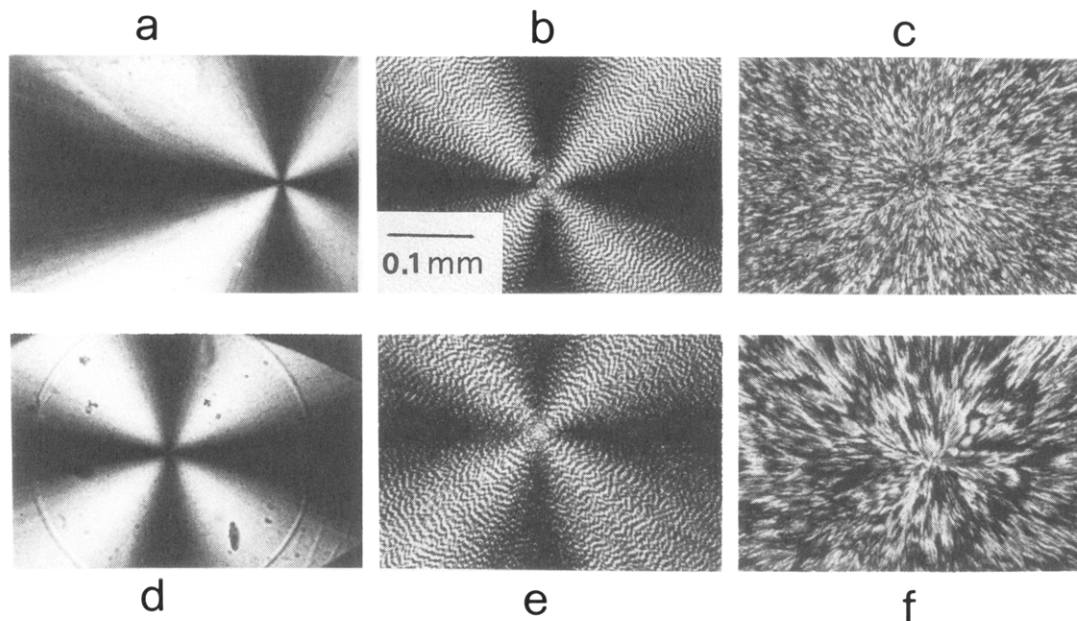


**Figure 4.** Optical micrographs (same magnification, bar = 0.1 mm) of (80/20) PHB/CE2 (upper row) and (84/16) PHB/CE1 (lower row) blends, isothermally crystallized at 70 (a, d), 90 (b, e), and 130 °C (c, f).

in Figure 3 are centered at about 90 °C, i.e., the same temperature as pure PHB. Conversely, when the amount of cellulose ester increases to 50% (see blend PHB/CE2 in Figure 3), the whole  $G$  vs  $T_c$  curve appreciably shifts toward higher temperatures, indicating that  $T_g$  gets closer to the lower limit of the investigated  $T_c$  range. In addition to the effect of dilution, it is likely that the crystallization rate depression of the 50/50 blend arises from high viscosity of the mixed melt, which decreases the segmental mobility of the crystallizing macromolecules.

Observation of the isothermally crystallized PHB/CE blends between the crossed polars of an optical microscope shows that the samples are completely filled with impinging spherulites. The spherulites display the "maltese cross" birefringent pattern as well as the circular extinction rings (bands) typically found in pure PHB. Figure 4 shows micrographs of blends containing 16% CE1 and 20% CE2 at three different  $T_c$ s (70, 90, and 130 °C). No apparent morphological differences appear in the micrographs attributable to substitution of CE1 with CE2 at these very similar compositions. On the other hand, a parameter which clearly plays a fundamental role in determining morphology is the crystallization temperature.

In agreement with a common finding regarding isothermally crystallized pure polymers—including PHB<sup>19,20</sup>—the micrographs of Figure 4 show that the distance between contiguous circular bands, i.e., the band spacing  $S$ , increases with increasing crystallization temperature in the blends too. Concomitantly, the spherulite texture becomes coarser and more open. Besides the mentioned effect of temperature, an additional parameter which affects spacing is blend composition. As an example, Figure 5 shows the dependence on composition of band spacing for PHB/CE1 and PHB/CE2 blends isothermally crystallized at two different temperatures (90 and 100 °C). At both  $T_c$ s,  $S$  decreases with increasing cellulose ester concentration, rather independently of the identity of the specific CE in the blend (whether CE1 or CE2). Moreover, at each individual composition the effect of temperature (larger  $S$  at higher  $T_c$ ) is confirmed. Though over a range of compositions more limited than that investigated in the present case, evidence of a decrease of band spacing with increasing concentration of the noncrystallizable

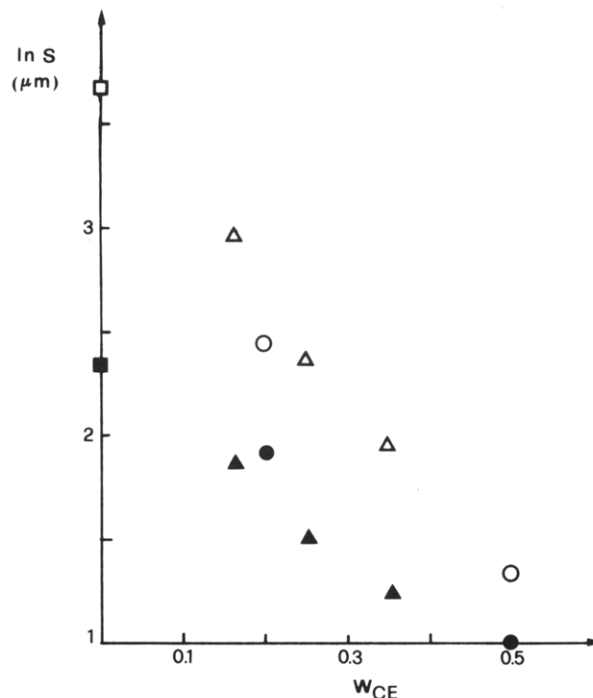


**Figure 5.** Dependence of band spacing on cellulose ester content, for spherulites of PHB/CE1 (triangles), PHB/CE2 (circles), and PHB (squares) crystallized at 90 °C (full symbols) and 100 °C (open symbols).

component has been previously reported in blends of poly(vinylbutyral) (0.2–15%) with poly( $\epsilon$ -caprolactone).<sup>23</sup>

As already mentioned, when the amount of CE in PHB/CE blends is increased to 50%, the two blend systems behave differently. While the blend containing CE2 at each of the crystallization temperatures investigated still develops rather regular spherulites which grow at a constant rate (the  $G$  values plotted in Figure 3), the corresponding blend with CE1 shows a rather complex behavior characterized by a most unusual type of nonlinear growth. It is worth noting, however, that at the  $T_c$ s where nonlinear growth occurs spherical entities are still seen to develop from the melt, whose radial growth can be monitored.

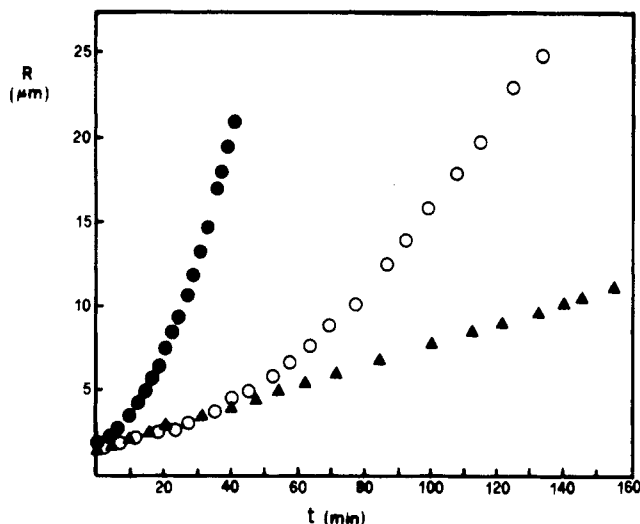


**Figure 6.** Spherulite radius as a function of time for a (50/50) PHB/CE1 blend at three crystallization temperatures: (▲) 65, (●) 95, and (○) 130 °C.

Representative radius vs time data for the (50/50) PHB/CE1 blend are collected in Figure 6. Three crystallization temperatures have been selected (65, 95, and 130 °C) which correspond, in the crystallization curve of the companion (50/50) PHB/CE2 blend shown in Figure 3, to low rate/low temperature, maximum rate, and low rate/high temperature crystallization conditions, respectively. At the lowest  $T_c$  reported in Figure 6, spherulites grow linearly with time from the melt, at a rate which favorably compares with that of the corresponding (50/50) blend in the other system (PHB/CE2) at the same  $T_c$ . In contrast to the normal behavior observed at  $T_c = 65$  °C, at the other two higher  $T_c$ s the data in Figure 6 show a remarkably departure from linearity, unambiguously indicating an increase of the crystallization rate with time. This behavior is very peculiar and—to our knowledge—has not been reported previously.

In the literature<sup>24,25</sup> examples can be found of binary blends composed of one crystallizable and one noncrystallizable polymer, where the diffusion rate of the noncrystallizable component is such that upon rejection during crystallization it migrates ahead of the growing front of the lamellae. As a consequence the composition of the melt changes, becoming richer in the rejected component. This compositional variation results in nonlinear growth of the spherulites, and—opposite to the present case—the rate is seen to decrease with time, due to a progressive decrease of concentration of the crystallizable component in the melt.

A way to rationalize the curvature shown by the data in Figure 6 (i.e., an accelerated growth of PHB spherulites from the molten blend) is to invoke a decrease of CE1 concentration in the melt as the process of PHB crystallization proceeds. The most likely reason for CE1 segregation from the mixed melt is the occurrence of crystallization of the cellulose ester. As a matter of fact, it was previously pointed out (see Figure 1) that CE1 is able to crystallize during DSC scans at 20 °C/min, provided the  $T_m$ – $T_g$  window is wide enough, the phenomenon being facilitated in the blends by the plasticizing action of PHB. In isothermal conditions it is rather obvious that CE1 crystallization will be further promoted. It is therefore highly likely that the change of slope observed in Figure 6 at  $T_c = 95$  and 130 °C is caused by segregation through crystallization of the cellulosic component from the mixed PHB/CE1 melt. This phenomenon occurs concomitantly

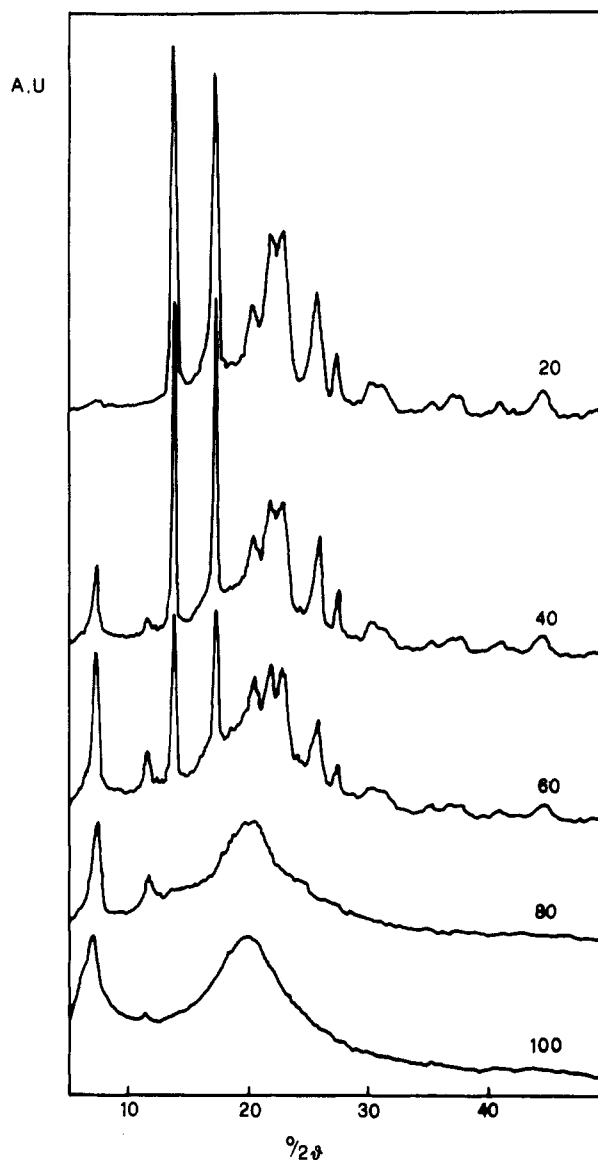


**Figure 7.** X-ray diffraction spectra of PHB/CE1 blends (number on curves: CE1 weight %).

to crystallization of the bacterial polymer, whose spherulite accelerated radial growth is shown in Figure 6.

The different behavior observed at the three  $T_c$ s reported is clearly due to changes in the relative crystallization rate of the two polymers. While at 65 °C the rate of crystallization of PHB—though quite low—must be higher than that of CE1, giving CE1 no chance to segregate from the melt before being trapped by the growing PHB lamellae, at 95 °C the continuous increase of curvature of the  $R$  vs time plot points to a progressive CE1 depletion in the melt during PHB crystallization. At this latter  $T_c$  therefore the crystallization rate of the two blend components should be comparable.

The case of  $T_c = 130$  °C is quite interesting, since after an initial curvature of the  $R$  vs  $t$  behavior, which extends up to about 80 min, the plot becomes linear, indicating that at  $t > 80$  min the PHB lamellae grow from a constant composition melt. The slope of the linear portion of the  $T_c = 130$  °C curve in Figure 6 falls in between the values of the isothermal crystallization rate (at the same  $T_c = 130$  °C) of PHB/CE1 blends containing 16 and 25% CE1 (see Figure 3). This finding suggests that, in this particular experiment on the 50/50 blend, two very different crystallization situations sequentially occur. At first the PHB spherulite grows in an accelerated fashion, during con-



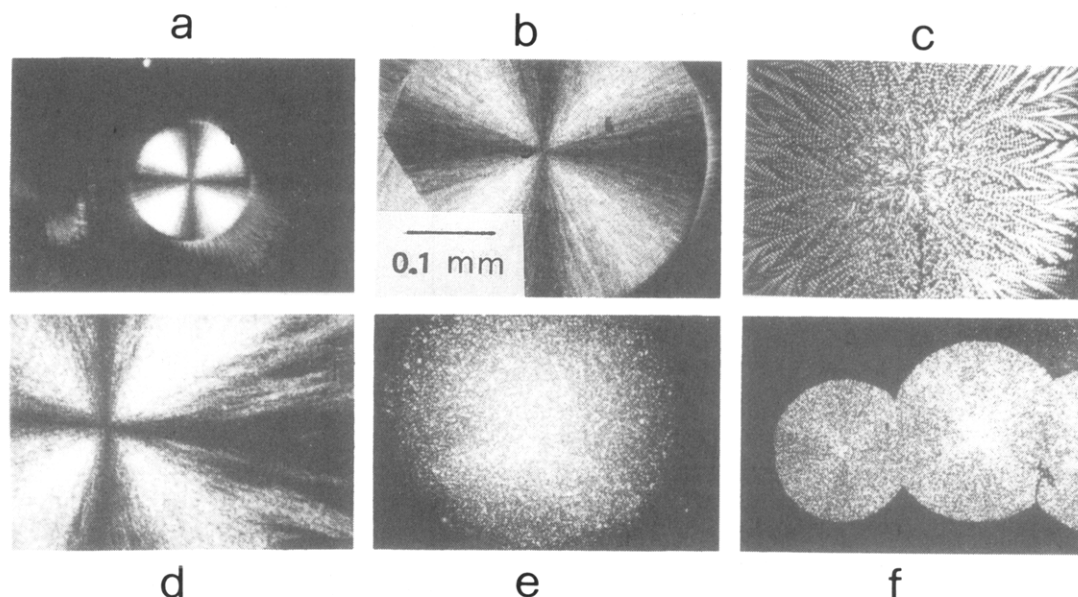


**Figure 8.** Optical micrographs of (50/50) PHB/CE2 (upper row) and PHB/CE1 (lower row) blends, isothermally crystallized at 65 (a, d), 90 (b, e), and 130 °C (c, f). Micrographs a, b, d, and e: same magnification (bar = 0.1 mm). Micrographs c and f: lower magnification ( $\times 0.16$ ).

comitant CE1 crystallization, up to a point where the melt becomes too poor in CE1 to allow any further crystallization of the cellulosic component. From the results of Figure 6, the mixed PHB/CE1 melt from which the cellulose ester stops crystallizing can be estimated to contain about 20% CE1. From this point on, crystallization of PHB proceeds in a regular way, i.e., at a constant rate from a constant composition melt.

The results (not shown) of isothermal crystallization experiments at 130 °C on a PHB/CE1 blend containing 60% CE1 confirm the above conclusions concerning the 50/50 blend. In particular, in the 40/60 PHB/CE1 blend, after an initial accelerated growth, the PHB spherulites are seen to reach a steady-state radial growth, whose rate closely matches that of the final portion of the  $R$  vs  $t$  plot of the 50/50 blend crystallized at 130 °C (Figure 6). The identity of the final growth rate indicates that, notwithstanding the different initial amount of CE1 in the two blends, the cellulose ester segregates through crystallization until the amount of CE1 in the melt is about 20%, this composition representing a limit to crystallizability of the cellulosic component in the experimental conditions employed.

In order to support the above suggestion of the concomitant crystallization of CE1 and PHB from certain blend compositions at given  $T_c$ s WAXS measurements were carried out on PHB/CE1 blends, allowed to crystallize isothermally from the melt in an oven at 120 °C for 100 h. The X-ray diffraction results are shown in Figure 7, where the spectra of pure CE1 and of blends with different compositions are shown. Comparison of the spectrum of the pure cellulose derivative with that of blend 20/80 shows that the addition of 20% PHB allows a more ordered crystalline CE1 phase to develop, as evidenced by the sharpness and intensity (relative to the broad reflection centered around  $2\theta = 20^\circ$ ) of the reflections at about  $7.3^\circ$  and  $11.5^\circ$ . When the amount of PHB increases to 40 and 60%, the diffraction spectrum of a PHB crystalline phase<sup>20</sup> appears with increasing evidence, superimposed to that of the crystalline CE1 phase. These results corroborate the foregoing discussion on the isothermal crystallization behavior of the (50/50) PHB/CE1 blend at high temperatures. Further support to the above interpretation comes

from the X-ray spectrum of the PHB/CE1 blend (80/20) shown in Figure 7, where no appreciable crystalline CE1 phase is observed, confirming that CE1 is unable to segregate through crystallization from CE1-poor melts and thus explaining the attainment of a steady-state growth upon depletion of the CE1 component in the melt (see  $T_c = 130$  °C in Figure 6).

Figure 8 compares the morphologies obtained from the two 50/50 blends examined (PHB/CE1 and PHB/CE2) upon isothermal crystallization in the microscope hot stage, at three representative temperatures (65, 90, and 130 °C). As already mentioned, the 50/50 blend containing the noncrystallizable cellulose ester CE2 develops regular spherulitic morphologies over the whole range of  $T_c$ s examined. Worth noting is the coarse and open texture with evident banding of the spherulite grown very slowly at 130 °C. In regard to the blend containing CE1, though no extinction bands are observed at any crystallization temperature investigated, the maltese cross is well evident in the spherulite grown at a constant rate at  $T_c = 65$  °C. On the contrary, the spherulites grown from this blend at 90 and 130 °C completely lack the characteristic extinction pattern. When the melt is observed during isothermal crystallization at the highest  $T_c$ s explored (120 and 130 °C) without insertion of the analyzer lens, the initially smooth melt is seen to become increasingly rough, but upon insertion of the analyzer no birefringence is observed. Birefringence appears only when a PHB spherulite grows on this uneven melt (see micrograph f in Figure 8,  $T_c = 130$  °C). Roughness of the melt is ascribed to formation of randomly oriented small CE1 crystals which at a later stage become included in the growing PHB spherulite. The absence of the common extinction patterns (maltese cross and banding) in the spherulites grown under these circumstances can be attributed to the disturbing role played by the CE1 crystalline phase on the growing process of PHB lamellae.

## Conclusions

The rate of isothermal crystallization of PHB has been found to be strongly affected by blending with the cellulose esters used in this work. PHB is miscible in all proportions in the melt with both CE1 and CE2 and develops space-

filling spherulites at all crystallization temperatures and compositions investigated: the spherulites grow to impingement, and no interspherulitic segregation of the CE component is observed. The rate of spherulite growth is strongly depressed by increasing amounts of cellulose ester in the blends: a decrease of  $G$  of 2.5 orders of magnitude is reached in the blend containing 50% CE2.

Composition and crystallization temperatures are the parameters which play a prominent role in determining morphology. The banded spherulites which grow from the molten blends show a band spacing that increases with  $T_c$  at constant composition, and decreases with increasing CE content at constant crystallization temperature.

In the range of CE contents 0–25%, both morphology and crystallization rate depression are rather independent of the identity of the cellulose ester (CE1 or CE2) in the blend. Only at higher CE contents do morphological differences—associated with the capability of one of the cellulose esters (CE1) to crystallize in certain experimental conditions—appear in the isothermally crystallized blends. The complex morphologies which develop in the (50/50) PHB/CE1 blend are mainly dictated by the different relative crystallization rates of the two components over the range of crystallization temperatures explored. A number of different situations generate during blend crystallization from the melt, ranging from the commonly expected steady-state spherulite growth at low  $T_c$ s to a very unusual accelerated growth at intermediate and high  $T_c$ s, caused by concomitant CE1 crystallization. At the highest  $T_c$ s explored the latter behavior is followed (at long crystallization times) by a recovery of the steady-state growth, which sets in when depletion of CE1 in the melt due to crystallization of the cellulose ester has decreased the concentration of CE1 to about 20%.

**Acknowledgment.** We thank Andrea Magni and Lara Finelli for performing the isothermal crystallization measurements and Gianpaolo Tomasi for the X-ray diffraction spectra. This work was partially supported by

CNR (Progetto Finalizzato Chimica Fine II) and by Ministero della Università e della Ricerca Scientifica e Tecnologica.

## References and Notes

- (1) Holmes, P. A. In *Developments in Crystalline Polymers*; Bassett, D. C., Ed.; Elsevier: New York, 1988; Vol. 2.
- (2) Anderson, A. J.; Dawes, E. A. *Microbiol. Rev.* **1990**, *54*, 450.
- (3) Doi, Y. *Microbial Polyesters*; VCH Publishers, Inc.: New York, 1990.
- (4) *Proceedings of the International Symposium on Bacterial Polyhydroxyalkanoates*; Schlegel, H. G., Steinbüchel, A., Eds.; Goltze-Druck: Göttingen, Germany, 1993.
- (5) Bhalakia, S. N.; Patel, T.; Gross, R. A.; McCarthy, S. P. *Polym. Prepr. (Am. Chem. Soc., Div. Polym. Chem.)* **1990**, *31* (1), 441.
- (6) Yasin, M.; Holland, S. J.; Jolly, A. M.; Tighe, B. J. *Biomaterials* **1989**, *10*, 400.
- (7) Kumagai, K. *Polym. Degrad. Stab.* **1992**, *36*, 241.
- (8) Dave, P.; Gross, R. A.; Brucato, C.; Wong, S.; McCarthy, S. P. in *Biotechnology and Polymers*; Gebelin, C. G., Ed.; Plenum Press: New York, 1991; p 53.
- (9) Avella, M.; Martuscelli, E. *Polymer* **1988**, *29*, 1731.
- (10) Greco, P.; Martuscelli, E. *Polymer* **1989**, *30*, 1475.
- (11) Holmes, P. A.; Newton, A. B.; Wilmouth, F. M. Eur. Patent N.52460, 1985.
- (12) Scandola, M.; Ceccorulli, G.; Pizzoli, M. *Macromolecules* **1992**, *25*, 6441.
- (13) Lotti, N.; Scandola, M. *Polym. Bull.* **1992**, *29*, 407.
- (14) Ceccorulli, G.; Pizzoli, M.; Scandola, M. *Macromolecules* **1993**, *26*, 6722.
- (15) Pizzoli, M.; Scandola, M.; Ceccorulli, G.; Piana, U. *Book Abstr.—4th Eur. Symp. on Polym. Blends*; **1993**, 309.
- (16) Lotti, N.; Pizzoli, M.; Ceccorulli, G.; Scandola, M. *Polymer* **1993**, *34*, 4935.
- (17) Fox, T. G. *Bull. Am. Phys. Soc.* **1956**, *1*, 123.
- (18) Wood, L. A. *J. Polym. Sci.* **1958**, *28*, 319.
- (19) Barham, P. J.; Keller, A.; Otun, E. L.; Holmes, P. A. *J. Mater. Sci.* **1984**, *19*, 2781.
- (20) Scandola, M.; Ceccorulli, G.; Pizzoli, M.; Gazzano, M. *Macromolecules* **1992**, *25*, 1405.
- (21) Keith, H. D.; Padden, F. J. *J. Appl. Phys.* **1964**, *35*, 1270.
- (22) Wang, T. T.; Nishi, T. *Macromolecules* **1977**, *10*, 421.
- (23) Keith, H. D.; Padden, F. J.; Russell, T. P. *Macromolecules* **1989**, *22*, 666.
- (24) Keith, H. D.; Padden, F. J. *J. Appl. Phys.* **1964**, *35*, 1286.
- (25) Tanaka, H.; Nishi, T. *Phys. Rev. A: Gen. Phys.* **1989**, *39*, 783.